Digital Rock Physics for Coreflooding Simulations

Mahesh Avasare
Masters in Petroleum Engineering, IST Lisbon | Intern, R&D Center, CEPSA

Experimental corefloodings have proved to be important tool for decades of research in oil exploration and production. Accurate and high quality coreflooding results are integral part for reservoir performance prediction and effective reservoir management. But achieving such high quality flooding measurements in the laboratory is by no means an easy task. In the past decade, Digital rock physics (DRP) has received attention better computational power, advanced scanning techniques and rise of EOR projects with depletion easy oil.

This work attempts to integrate DRP into a dynamic coreflooding simulation. It explains details of development steps and also includes few sensitivity analysis studies with the model. The resulting reference model helps to qualitatively understand uncertainties involved in simulation results with respect to experimental coreflooding. This work has been developed at R&D Center of CEPSA (Madrid), in association with E&P division of CEPSA.

Keywords: Digital Rock Physics, Coreflooding Simulations, Coreflooding Uncertainties

---

1. Introduction

In the era of low oil prices, economic viability of oil fields strongly relies on accurate technical analysis and predictions. Detailed core analysis is one of the most reliable information about in-situ conditions. After extracting petrophysical properties with core characterization, corefloodings are performed to evaluate dynamic fluid responses by cores. This work has formalized a method to understand and tackle uncertainties associated with coreflooding results.

Generally the cores possess local micro-heterogeneities. Patterns of preferential path of flow are distinctly visible when cores are split opened after flooding. Such heterogeneities cause deviation from expected behavior of the flooding. As a result, properties or techniques predicted through corefloodings might be misleading. To avoid such uncertainties, computational simulation of corefloodings can be performed along with experimental floodings.

This work explains detailed development steps of coreflooding computational model in association with Digital Rock Physics. Static model for this simulation is based on computed tomography (CT) scan results; whereas the dynamic model is developed with a black-oil simulator. With sensitivity analysis of various parameters, boundary conditions have been tested too.

Stepwise dynamic coreflooding model development has been explained in this paper. History matching has been performed by altering mainly the local permeability distribution and relative permeability curves. The reference model developed achieved good results within the boundaries of established simulation constraints.

Till date, only few industry giants are involved into similar study. The companies can use output of DRP based simulations as input to numerical reservoir simulators, fracture design programs etc.; which will improve reserve forecasts, rate of forecasts, well placement and completion designs. With potential to improve efficiency of oil industry, this technology will surely have a bright future ahead.

2. Corefloodings

After extracting petrophysical properties with core characterization, corefloodings are performed to evaluate fluid behaviors in the given core or plug. Also the production methodologies are tested on plugs to predict the response of the reservoir. Due to relatively higher certainty on the results from coreflooding, it is one of the most important source of petrophysical data for reservoir engineering.

The cores from field can have local geological heterogeneities; originating from in-situ heterogeneity or improper core extraction and transportation methods. Due to such heterogeneities, experimental tests show deviation from real results. To minimize such uncertainties, computational simulation of corefloodings will be helpful tool.

2.1 Uncertainties in Corefloodings

- Unrepresentative of in-situ conditions:
  - During extraction or transportation, core's petrophysical properties might be modified
  - Evaporation of light components or asphaltenes precipitation will change fluid properties
  - Cleaning and aging can alter rock-fluid interactions (like wettability)
- Limitations in up-scaling to reservoir level
  - High geological-variability inside reservoirs decreases certainty of petrophysical properties extracted from core to large geological area in the reservoir
  - Up-scaling of EOR methodologies is limited with many external parameters like raw material availability, govt. rules, economic profitability, on field consistency etc.
  - Huge difference in modeling scale from core to reservoir possesses technical challenges
- Experimental Errors
  - Minute errors from lab setup create high impact on results due to small size of plugs

3. Digital Rock Physics

Main objective for use of Digital Rock Physics (DRP) methodology is to understand local micro-heterogeneities across the core. Without the understanding of local heterogeneities, the averaged properties calculated from core analysis can increase uncertainty in reservoir calculations.

Digital Rocks are generated by Computerized Tomography (CT) scanning of the core. Internal structure of the core is recreated with imaged cross-sectional slices. The final model is reconstructed from matrix of X-ray attenuation coefficients (Hunt, 1988). Normally the plugs are scanned at a resolution of 500 microns (Kalam, 2012). The attenuations are based on measurement of reduction of X-rays' intensity, due to transmission through the object at certain coordinates. As a result, this attenuations can be translated into local density distribution. Further density model can be translated into porosity-permeability models with some uncertainty.

3.1 DRP Output: Case Study

This case study has been performed at R&D center of Compañía Española de Petróleos, S.A.U. (CEPSA). For simulations, ECLIPSE 2014.1 (black oil simulator) and PETREL 2013 (reservoir simulator) were used with a core from Caracara Sur Field in Colombia.

Caracara Sur field (CCS) is located at the south west of Llanos Foreland basin (Bozorgzadeh, et al., 2015). The producing formation in the CCS field is the early Oligocene Carbonera-7. The CCS consists of multilayered compartmentalized fluviodeltaic reservoirs (Cubillos, et al., 2013)

Plug 184 from CCS was chosen as a case study for this work. Results of the CT Scan for the Plug 184 can be summarized as:

- Model Geometry: Orthogonal Grid
- Model dimensions: 35.4x35.4x50.6 mm
- CT scan resolution: 500x500x625 µm
- Total number of grid cells 408k
- Active number of grid cells 316k
- Z direction lies along the axis of the core
- X and Y directions are arbitrary

Note: The model, as shown in Figure 1, is achieved after several processing steps on the raw data.

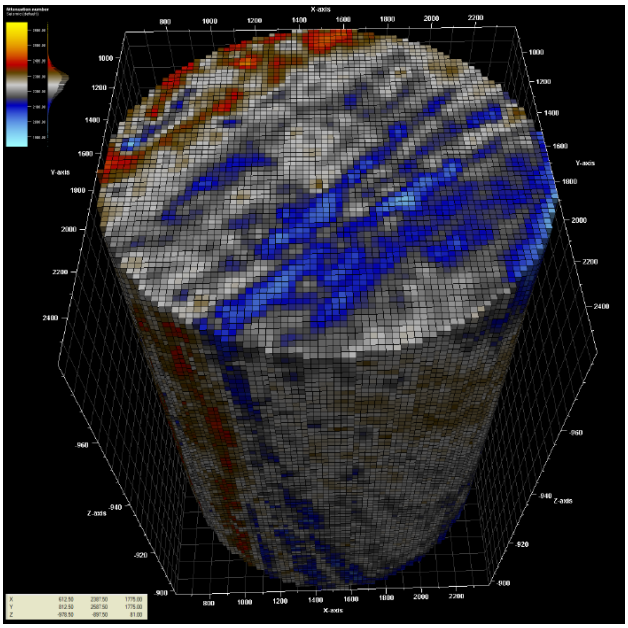

Figure 1 Processed CT Scan Results (Attenuations)

4. Coreflooding Simulation with DRP: Goal, Methods & Constrains

Due to high simulation time and wide scope of tuning various parameters, a clarified base of simulation goals, methodology to be followed and constraints to be followed is necessary.

4.1 Simulation Goal

The goal of the work is to generate a set of relative permeability curves representative of field behavior; which can be further utilized in full scale field models. This can be achieved by history matching global and local trends of dynamic simulation model with experimental findings.

4.2 Simulation Methods

- History matching for oil production profile.
  *(As the **end-effect**[#] generated in experimental coreflooding cannot be reproduced completely in the ECLIPSE simulations, the exact history match cannot be achieved. But the profile trend and approximate profile range should be achieved.)*
- Regenerating of pressure gradient range across the core.
  (Pressure gradient trend generated in laboratory does not follow physical phenomenon. So complete regeneration of this trend is impossible too.)
- Apart from the above global history match, history matching is done to regenerate local trends. *(Local trends include oil un-swept zones and zonal water saturation. Oil un-swept zones, as seen after coreflooding in lab, is generated in dynamic model. Zonal water saturation, as measured with XRD, is reproduced by dynamic model too.)*

4.3 Simulation Constraints

- End points of reference relative permeability curve are obtained using multiple laboratory experiments on numerous plugs from the reservoir. So, end points of the relative permeability curve should not be altered, unless specified in the model.
- Multiple relative permeability curves should be generated by adjusting corresponding *Corey Exponents*. As the exponents lie in theoretical range of 1 to 5 (Corey, et al., 1956), all following models are developed accordingly.
- Apart from permeability distribution, other static models have high certainty. So other parameters of static models should not be modified during the study.

Note: All models developed below follow constrains defined above, unless and until mentioned.

'End Effect' arises from pressure gradient across two phases in the plug; compensated with capillary forces to achieve equilibrium at production outlet. Therefore it is also known as "Capillary End Effect" (Arne Skauge, 2001). Though it is a very important phenomenon for corefloodings, due to high complexity, this study does not address the phenomenon.

5. Development of 3D Static Model

A reference model was developed, starting from CT Scan results of the Plug 184 from CCS field, as defined in 3.1 DRP Output: Case Study. A base static model is developed with following steps:

5.1 Attenuation Model to Density Model

Analytical correlation was established by E&P division of CEPSA with average attenuation of complete plug and bulk density of the plug.

Data of 10 plugs for average attenuation vs average density showed highly linear trend (R^2 = 0.96). The Plug 184 showed a close match to this trend line, as shown in Figure 2.

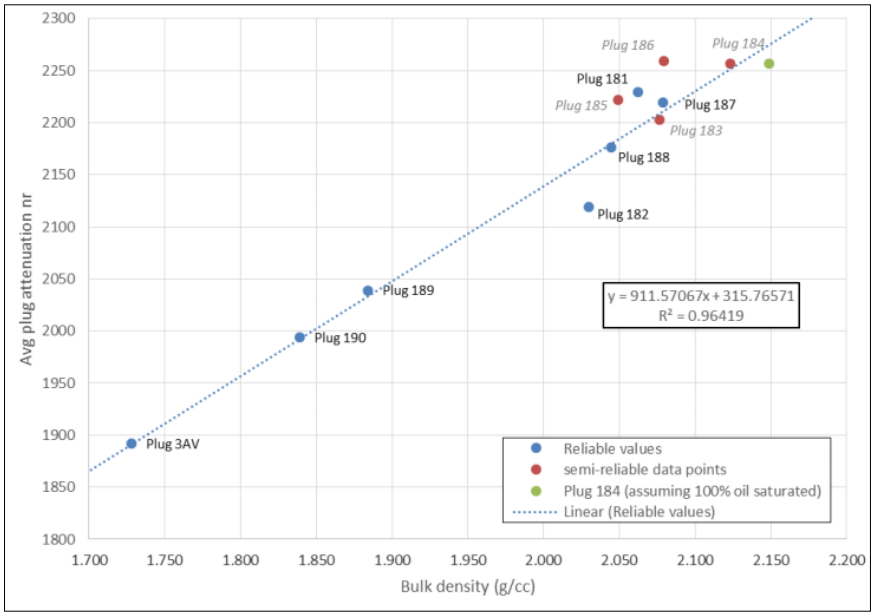

Figure 2 Correlation of Avg. Attenuation & Avg. Density (Courtesy: E&P, CEPSA)

The plug model was transformed from attenuation distribution to density distribution with following equation, as extracted from Figure 2.

$$Attenuation\ (i,j,k) = 911.5706 * Density(i,j,k) + 315.7657 \quad \ldots(1)$$

5.2 Density Model to Porosity Model

The plug is assumed to be made of '*Grain*' particles & '*Fluid*' particles. Where, *Fluid* is assumed to be mixture of oil, water and air. From *Routine Core Analysis*, average density of the *fluid* was calculated [$\rho_{Fluid} = 0.84$ gm/cc]. *Grain* mainly consists of Quartz [$\rho_{Quartz} = 2.65$ gm/cc] and minor quantities of other sand and asphaltenes. *Grains* density was calculated with weighted average of the constituents' density [$\rho_{Grain} = 2.60$ gm/cc].

Local porosity was determined with a simple assumption of all pore spaces are occupied by *fluids*; and rest of the plug volume is occupied by *Grains*. The simplified correlation can be equated as:

$$\text{Porosity } [\Phi\ (\mathrm{i,j,k})] = 1 - \frac{\rho(i,j,k) - \rho_{\mathrm{Fluid}}}{\rho_{\mathrm{Grain}} - \rho_{\mathrm{Fluid}}} \quad \ldots(2)$$

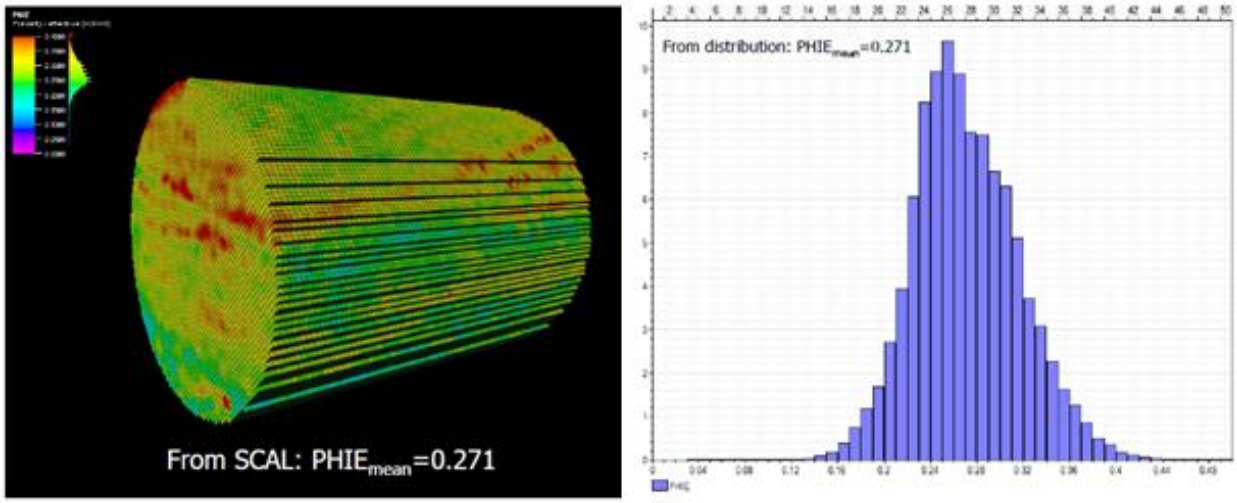

Figure 3 Porosity Model Generated & Corresponding Univariate Distribution

Mean porosity of the model generated closely matched with experimental porosity distribution. This verifies calculations and assumptions made till this point.

5.3 Porosity Model to Permeability Model

As permeability does not follow simple arithmetic or geometric correlations, it can only be modelled with data-backed correlations with other petrophysical properties. *Mercury Injection Test* on plugs gives pore size distribution from graph of injection pressure vs pore volume saturation (Lenormand, 2003).

Following steps was implemented to build permeability model:

- On the basis of pore throat distribution with mercury injection test, all the plugs from Caracara field are divided into 4 '*Rock Types*' (RT1, RT2, RT3 and RT4).
- RT1 being most permeable (in range of 5D) to RT4 being the lowest permeable (in range of 50 mD).

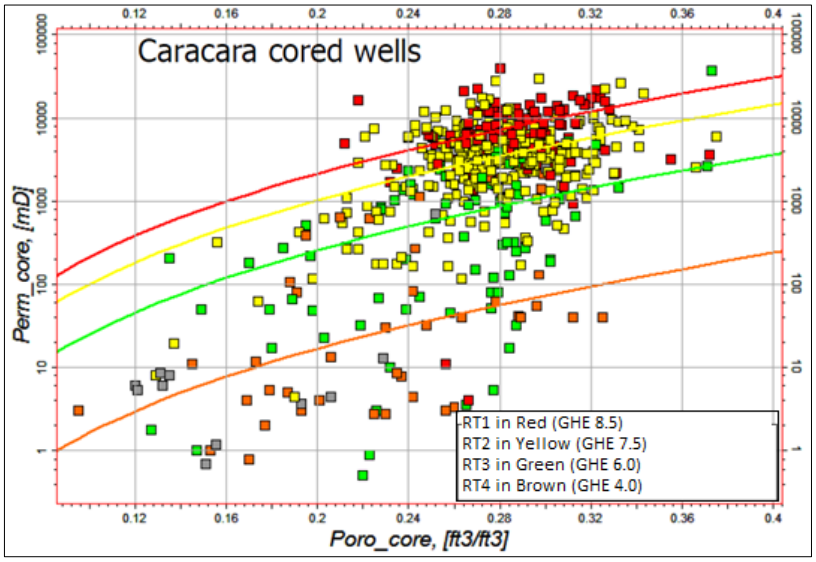

Figure 4 Permeability vs Porosity Correlation with Rock Type Classification

- As shown in Figure 4, these rock types showed different polynomial trend lines between permeability (log-scaled) and porosity. The Plug 184 was classified into RT2 according to pore size distribution. So the trend line of RT2 was used to generate permeability model from porosity model.

6. Development of 3D Dynamic Model

Static base model developed in PETREL® by combining porosity and permeability models, is further modified to attain a dynamic base model representative of experimental conditions in ECLIPSE®. Few of the important steps for the dynamic base model development as follows:

Injection Geometry Integration	The experimental coreholder has an injection head with symmetric thin grid spreading injection water equally over the injection face. This geometry is replicated with an injection well connecting all blocks on injection face.
Simulation Optimization	Due to geometrically fine grid and limited computational power, the simulation time became an important parameter to be optimized. A time-step scheme is developed with least number of simulation errors and practical simulation time.
Assigning Relative Permeability Curve	Relative permeability curve plays an important role in oill drainage by the plug during coreflooding. After due scrutanization, relative permeability curve used by CEPSA for CSS field simulation (Kr_CEPSA), was assigned for base case.

A base dynamic model developed by this stage, was further modified to attain better history match with experimental coreflooding results. History matching is performed only by tweaking relatively most uncertain parameters in the model: relative permeability (kr) curve & permeability distribution.

6.1 History Matching with Permeability Distribution Model

Permeability distribution model, as show in Figure 5, show unimodal distribution. As observed from experimental coreflooding, the plug show high local hetrogenity.

To replicate the local hetrogenity, initial attempts were made to increase standard deviation of the permeability model. This was achieved by cokriging the distribution with another reference distribution of higher standard deviation.

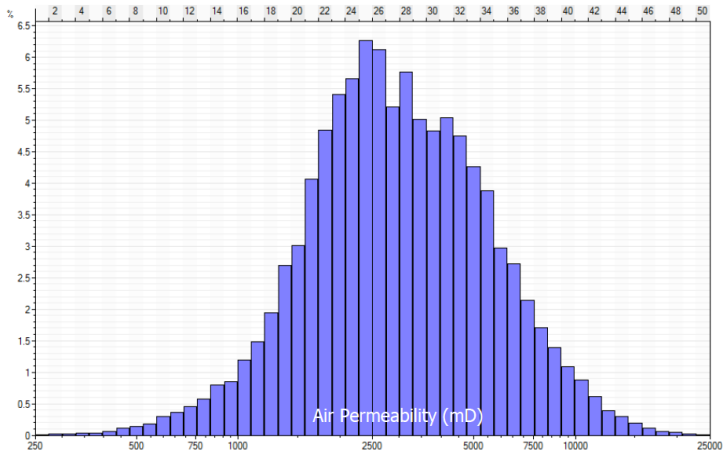

Figure 5 Permeability Model Distribution Histogram

It was expected that due to lower permeability zones, total oil production will drop. But the oil production curve showed almost similar trend despite increasing the permeability by 50%. In fact the water saturation distribution showed almost uniform sweeping. This established the fact that unimodal distribution, even with high standard deviation cannot replicate the experimental conditions.

As detailed in *5.3 Porosity Model to Permeability Model*, the plug was categorized into Rock Type 2. This assumption of homogenous composition in the plug was averaging out the heterogeneities arising due to other rock types.

The permeability model was redeveloped with all four porosity-permeability correlations, as shown in the Figure 4. On the basis of rock types composition of in the reservoir, porostiy cutoffs were made & corresponding correlation segments were used.

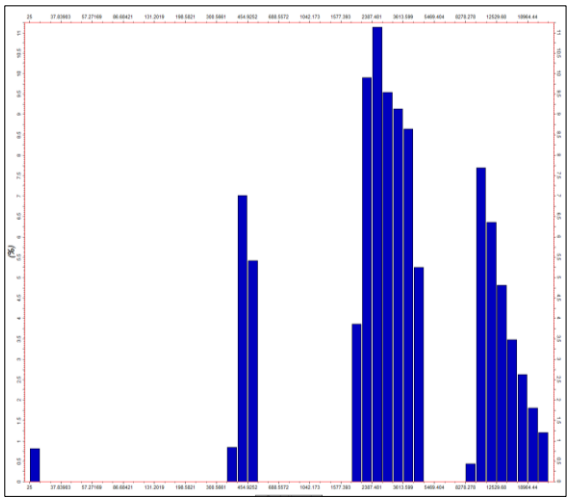

Figure 6 Modified Permeability Distribution

Resulting permeability distribution, as in Figure 6, showed 4 peaks corresponding to each rock type.

6.2 History Matching with Relative Permeability Curve

Initial attempts were made with extremities of *Corey Exponents*. It was noticed that alterations in Corey Exponents can affect cumulative oil production significantly, but overall sweep pattern remains the same. Similarly, during attempts with alterations in *relative water permeability at residual oil saturation (Krw,ro)*, homogenous sweeping pattern persisted. Also cumulative oil production dropped by less than 5% for doubled Krw,ro with respect to base case.

To generate heterogeneities across the plug, different relative permeability curves were assigned to different rock types generated above. As explained in section *5.3 Porosity Model to Permeability Model*, RT1 is the most permeable rock type whereas RT4 is least permeable.

To integrate this phenomenon into the dynamic model, residual oil saturation was varied from 0.23 from RT1 to 0.5 for RT4. Also, water permeability at residual oil saturation increased from 0.24 for RT1 to 0.6 for RT4.

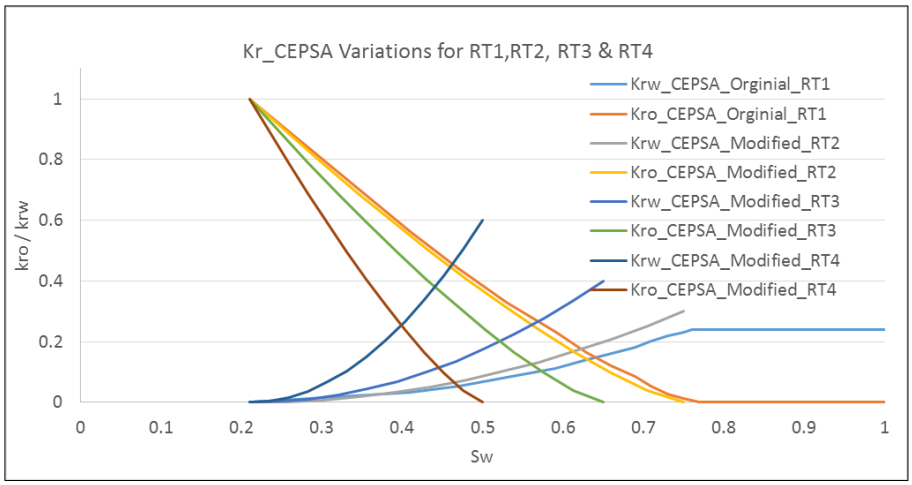

Figure 7 Different Kr curves for different Rock Types

This increased the contrast between oil retention capabilities among the rock types. Resulting relative permeability curves are summarized in Figure 7.

7. Reference Model and Sensitivity Analysis

A reference model was developed with permeability distribution as shown in Figure 6, and set of relative permeability curves as shown in Figure 7. All other parameters are also within bounds of experimental data. So the complete dynamic model is a representative of experimental coreflooding conditions.

The simulation output showed un-swept oil zones. But the cumulative oil production was at higher level than the experimental findings. One of the important reasons of lower oil production in laboratory experiment is the strong *capillary end effect* in the Plug 184. Dynamic saturation profile comparison is summarized in Figure 8. Lab saturation profile also verifies capillary end effect in the plug.

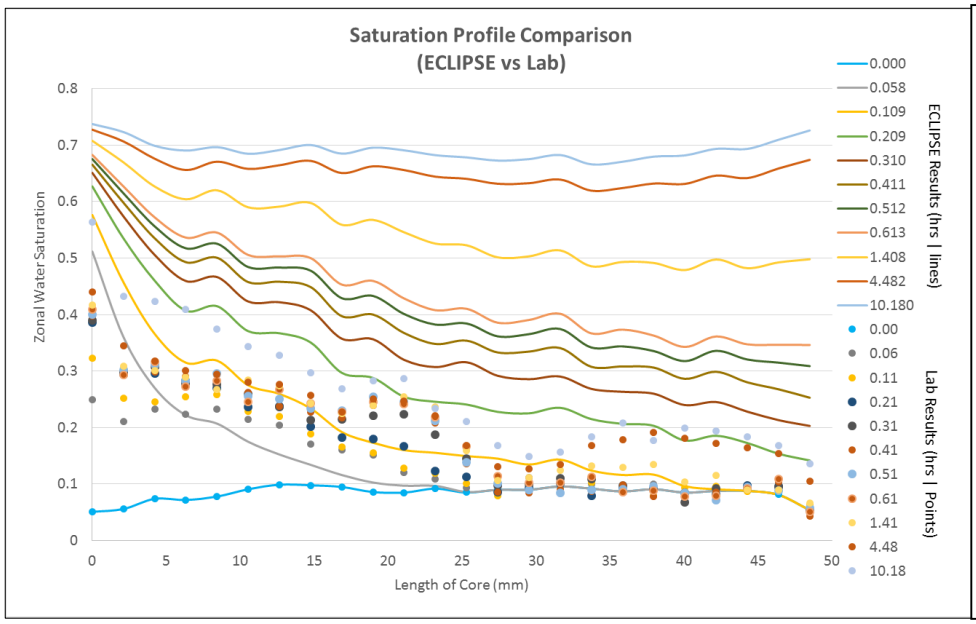

Note: Each line or a dot, represent corresponding saturation at given time (hours), as represented in right hand side of the chart. Though results from experiment as well as lab have more time steps, only few time steps are shown here.

Figure 8 Zonal Water Saturation Profile Comparison (Reference Model vs Lab Data)

Though the simulation model could not completely match saturation trends observed in the lab, overall simulation results recreate gist of the laboratory response by the plug.

7.1 Sensitivity Analysis on 3D Dynamic Model

One of the sensitivity analysis was realized by varying wettability of the core. As RT1 and RT2 constitute to majority of the plug, the wettability was altered majorly for RT3 and RT4, as visible in Figure 9.

Due to increased water wet behavoir, oil recovery dropped by 7% from reference model. So wettability can alter plug response notably.

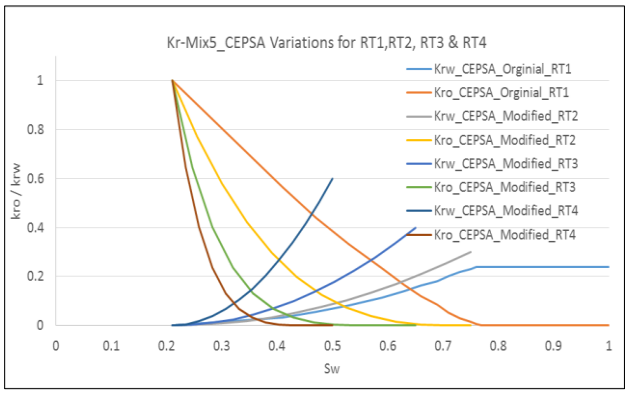

Figure 9 Modified Kr Curve for Sensitivity Analysis

Another sensitivity analysis was performed by altering injection geometry. In this analysis, small square injection face was assumed, as shown in Figure 10; instead of complete face injection as in

Oil production was not altered notably, despite reducing injection face upto 10 fold. This shows that the plug has high radial mobility for water near the injection face.

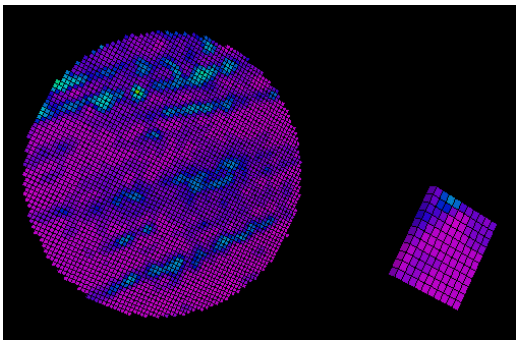

Figure 10 Injection Geometry Sensitivity Analysis

8. Conclusion and Future Suggestions

Initial literature survey about integration of Digital Rock Physics into coreflooding simulations showed high potential of the technology as a future alternative to laboratory core analysis. Rapid rise of the technology in the past decade can be attributed to higher computational power, advanced scanning techniques and rise of EOR projects with depleting easy oil.

Development of the static model showed high complexity attributed to petrophysical property distribution, especially the permeability distribution. After setting up simulation goals and constraints, framework for dynamic model development was chalked out. History matching was done in reference of lab data, by varying permeability distribution and relative permeability curves.

The reference model developed post history matching could not completely reproduce experimental trends, as some experimental attributes were not integrated into the simulation; like capillary end effect. Further sensitivity analysis showed extremity effects for parameters like injection area, wettability etc.

Bibliography

Arne Skauge Trond Thorsen, Andre Sylte Rate Selection For Waterflooding Of Intermediate Wet Cores [Conference] // International Symposium of the Society of Core Analysis. - Norway : SCA, 2001. - Vol. 20.

Bozorgzadeh M., Romero Fernandez Pedro e Rodriguez Rosario Calibrating a Field-Scale Numerical Simulation Study for the Implementation of a Chemical Enhanced Oil Recovery Pilot Using Core Flooding [Conference] // SPE Reservoir Characterisation and Simulation Conference and Exhibition. - Abu Dhabi, UAE 2015

Corey A.T. e Rathjens C.H. Effect of Stratification on Relative Permeability [s.l.] : Journal of Petroleum Technology, 1956. - 12 : Vol. 8.

Cubillos H., Stofferis M. e Vanegas G. Strategy and Planning EOR for Caracara Sur Field, Colombia [Conference] // EAGE Annual Conference & Exhibition incorporating SPE Europec. - London, UK : Society of Petroleum Engineers, 2013.

Hunt Patricia K. Computed Tomography as a Core Analysis Tool: Applications, Instrument Evaluation, and Image Improvement Techniques [s.l.] : Journal of Petroleum Technology, 1988. - 88 : Vol. 40.

Kalam Mohammed Zubair Digital Rock Physics for Fast and Accurate Special Core Analysis in Carbonates // New Technologies in Oil & Gas Industry. - [s.l.] : InTech, 2012.

Lenormand R. Interpretation of mercury injection curves to derive pore size distribution [Conference] // Internatio nal Symposium of the Society of Core Analysts. - Pau, France : [s.n.], 2003.

Orsi Thomas, Edwards Carl e Anderson Aubrey X-Ray Computed Tomography; a non-distructive method for quantitative analysis of sediment cores [Diário]. - [s.l.] : Journal of Sedimentary Research, 1994